Subcortically generated movements activate motor cortex during sleep and wake in rats through postnatal day 24

Madilyn R. Reid[1], James C. Dooley[1,2†‡]

[1]Department of Biological Sciences, Purdue University, West Lafayette, Indiana
[2]Purdue Institute for Integrative Neuroscience,
Purdue University, West Lafayette, Indiana

[†]Corresponding author: James C. Dooley, Ph.D. (jcdooley@purdue.edu)
[‡]Lead Contact: James C. Dooley

Keywords: Primary motor cortex, development, sensorimotor, REM sleep, myoclonic twitching, red nucleus, rat

Abbreviated title: Movement-related activity in developing M1

Abstract

During early postnatal development, cortical motor control emerges from complex interactions between cortical and subcortical circuits. In primary motor cortex (M1), we know that this process depends on neural activity, but large gaps remain in our understanding of how M1 neural activity is patterned prior to the development of cortical motor control. To track the development of movement-related activity in M1 across sleep and wake, we performed acute, extracellular recordings of single-unit activity in the forelimb region of M1 of unanesthetized, head-fixed rats from postnatal day 12 (P12) to P24. At all ages, a subset of M1 neurons responded robustly and somatotopically to spontaneous limb twitches that occur during REM sleep. M1 neurons also showed robust responses to wake movements at these ages. From P12 to P24, the proportion of M1 neurons that showed twitch-related activity decreased, twitch-related activity became more temporally refined, and there was an increase in the proportion of activity that preceded movement onset. To compare M1's developmentally nascent activity at P24 with that of an established motor structure, we performed simultaneous recordings in M1 and the red nucleus (RN). RN activity reliably preceded both twitches and wake movements, particularly compared to M1, reinforcing the conclusion that as late as P24 RN still predominantly drives limb movements. These results highlight M1's protracted development and the continued importance of subcortically generated movements in driving activity that shapes M1's circuitry, suggesting that movement-related activity during sleep and wake promotes the development of M1's motor functions.

Introduction

In placental mammals, primary motor cortex (M1) is viewed as the key player in movement production and motor learning (see Peters et al., 2017). However, it is increasingly apparent that motor control results from coordinated activity of the entire sensorimotor network, including the thalamus, basal ganglia, cerebellum, and brainstem motor nuclei (Kawai et al., 2015; Sauerbrei et al., 2020; Ruder et al., 2021; Inagaki et al., 2022; Lopez-Virgen et al., 2023; Yang et al., 2023). The contributions of these subcortical structures are impossible to ignore in infancy, as M1 is not yet capable of driving movement (Martin, 2005; Young et al., 2012; Williams and Martin, 2015; Singleton et al., 2021). Instead, in numerous mammals, including rats, limb movements are primarily generated by brainstem motor nuclei, with the red nucleus (RN) of the midbrain playing a crucial role throughout this period (Rio-Bermudez et al., 2015; Williams and Martin, 2015).

But the developing M1 is not silent, as it responds to sensory feedback from self-generated movements (Dooley and Blumberg, 2018; Glanz et al., 2021; Gómez et al., 2021). Prior to postnatal day 10 (P10), the sensory feedback resulting from wake movements is actively inhibited in M1 (Tiriac et al., 2014; Tiriac and Blumberg, 2016). Thus, it is particularly responsive to myoclonic twitches produced throughout periods of REM sleep. This pattern is not unique to M1, as similar inhibition of sensory feedback during wake movements has been observed in primary somatosensory and visual cortex at these ages (Mukherjee et al., 2017; Murata and Colonnese, 2018; Dooley et al., 2020). This early sensory feedback drives and patterns a large proportion of early neural activity (Dooley and Blumberg, 2018; Dooley et al., 2020) throughout the period that this activity is necessary for the development of M1 motor control (Chakrabarty and Martin, 2005). Thus, this period of twitch-driven activity lays the groundwork for the development of M1's eventual motor functions.

As development progresses, M1 gradually assumes its role in motor control, which begins to emerge in rats around P25 and appears adult-like around P60 (Young et al., 2012; Singleton et al., 2021). This process is highly dependent on neural activity (Chakrabarty and Martin, 2005; Yang and Martin, 2023), as chronic inhibition of M1 at these ages not only impedes the development of cortical motor control but also alters the maturation of subcortical motor structures (Williams et al., 2014; Williams and Martin, 2015). However, little is known about the patterning of M1 neural activity prior to the onset of cortical motor control, nor how M1 neural activity compares to established structures like RN.

Here, we perform extracellular recordings in the forelimb representation of M1 in unanesthetized rats spanning P12 to P24 as they cycle between NREM sleep, REM sleep, and wake. This developmental window includes temporal refinement of thalamic inputs to M1 and the developmental emergence of cerebellar-dependent internal models (Dooley et al., 2021). By analyzing movement-related activity in M1 during both sleep and wake, we show that neurons in M1 respond to REM-sleep associated twitches and wake movements at all ages (P12 to P24). Taking advantage of the somatotopic discreteness of twitches, we show that neurons in the forelimb region of M1 respond exclusively to forelimb movements at all ages. Thus, sensory responses in M1 are somatotopically refined by P12. However, even at P24, movement-related activity in M1 does not systematically precede twitches or wake movements, suggesting that M1 is not yet

involved in generating movement. Finally, to compare M1 neural activity with an established motor structure, we performed simultaneous extracellular neural recordings in M1 and RN of P24 rats. We found that activity in RN systematically precedes twitches and wake movements, while M1 activity lags RN. Altogether, these results suggest that twitches drive somatotopically precise patterns of neural activity through P24 and that self-generated movements during sleep and wake strongly drive M1 activity. Yet even in weanling-aged rats, forelimb movements are still generated by RN.

Materials and Methods

Code Accessibility

All original code will be deposited at https://github.com/jcdooley/XXX upon publication.

Any additional information required to reanalyze the data reported in this paper is available from the corresponding author upon request.

Experimental model and subject details

For the first experiment, neurophysiological recordings of M1 were obtained from Sprague-Dawley Norway rats (*Rattus norvegicus*) at P12 (N = 9 pups; 30.8 ± 2.4 g; 3 male), P15-16 (hereafter P16; N = 12 pups; 43.7 ± 3.0 g; 8 male), P18-P20 (hereafter P20; N = 12 pups; 56.1 ± 4.4 g; 7 male), and P22-P24 (hereafter P24; N = 8 pups; 68.5 ± 4.7 g; 6 male). Animals within the same age group were always from different litters. Although the focus here is on M1 activity, recordings were performed in the forelimb region of M1 and either the ventral lateral or the ventral posterior nucleus of thalamus, and the thalamic data have been published and described previously (Dooley et al., 2021). For the second experiment, dual neurophysiological recordings were performed in M1 and the RN at P24 (N = 7 pups, 65.8 ± 5.2 g; 3 male). To be included in the analysis, animals needed more than 40 right forelimb twitches and at least one neuron had to be responsive to right forelimb twitches, criteria that led to the exclusion of 2 animals.

Pups were born and raised in standard laboratory cages (48 × 20 × 26 cm) in a temperature- and humidity-controlled room on a 12:12 light-dark cycle, with food and water available ad libitum. The day of birth was considered P0 and litters were culled to eight pups by P3. All pups had at least four littermates until P12 and at least two littermates on the day that neurophysiological recordings were performed. No pups were weaned before testing. All experiments were conducted in accordance with the National Institutes of Health (NIH) Guide for the Care and Use of Laboratory Animals (NIH Publication No. 80–23) and were approved by the Institutional Animal Care and Use Committee at the University of Iowa and Purdue University.

Method Details

Surgery. As described previously (Dooley et al., 2021), a pup with a healthy body weight and (for P12 pups) a visible milk band was removed from the litter and anesthetized with isoflurane gas (3–5%; Phoenix Pharmaceuticals, Burlingame, CA). The hair on the top of

the head was shaved and care was taken to ensure that the vibrissae were intact. For sleep/wake state determination, two custom-made bipolar hook electrodes (0.002-inch diameter, epoxy coated; California Fine Wire, Grover Beach, CA) were inserted into the nuchal and biceps muscles contralateral to the neural recordings. Carprofen (5 mg/kg SC; Putney, Portland, ME) was administered as an anti-inflammatory analgesic.

The skin above the skull was carefully removed and an analgesic (bupivicane; Pfizer, New York, NY) was applied topically to the skull. The skull was then dried with bleach. For P20 and P24 rats, any bleeding around the skull was cauterized to ensure that it was completely dry prior to the application of a headplate. Vetbond (3M, Minneapolis, MN) was then applied to the skin surrounding the incision, and a custom-manufactured head-plate (Neurotar, Helsinki, Finland) was secured to the skull using cyanoacrylate adhesive.

A trephine drill (1.8 mm; Fine Science Tools, Foster City, CA) was used to drill a hole into the skull above the forelimb representation of M1 (0.5 mm anterior to bregma, 2.2–2.5 mm lateral to the sagittal suture). When thalamic recordings were also performed (as reported in Dooley et al., 2021), a second hole was drilled above thalamus (2.0–2.8 mm caudal to bregma, 2.2–2.5 mm lateral to the sagittal suture). In Experiment 2, when RN recordings were performed, a second hole was drilled above RN (5.2 mm caudal to bregma, 0.4 to 0.8 mm lateral to the sagittal suture). A small amount of peanut oil was applied to the dura to prevent desiccation of the underlying tissue. This surgical procedure lasted approximately 30 min.

While recovering from anesthesia, the pup was secured to a custom-made head-fixation plate secured to a Mobile HomeCage (NTR000289-01; Neurotar). The height of the pup's head off the floor was adjusted depending on its age so that, when the pup was exhibiting atonia during active sleep, its body rested on its elbows (P12: 35 mm; P16: 38 mm; P20 and P24: 40 mm). EMG wires were carefully secured behind the pup's back to ensure that they would not get tangled. Pups recovered from anesthesia within 15 minutes and were acclimated to the head-fix apparatus for 1 to 2.5 hours. This period of acclimation allowed the recording electrodes to stabilize and the return of normal spiking activity (Domínguez et al., 2021). When recording began, all pups were exhibiting typical behavioral and electrophysiological features of sleep and wake (i.e., twitching, grooming, locomotion).

Recording Environment. Electrophysiological recordings were performed in a Faraday cage illuminated by flicker-free red LEDs (630 nm; Waveform Lighting, Vancouver, WA). Continuous white noise (70 dB) was present throughout the recording session. To maximize REM sleep, the room's temperature was maintained between 26.5 and 29° C (Szymusiak and Satinoff, 1981). The animal's head was positioned away from the entry to the room so that it could not see the experimenter entering or leaving, which was infrequent. For the comfort of both the experimenter and the subject, the experimenter was outside the room and monitoring the animal and data acquisition remotely.

Electrophysiological Recordings. The nuchal and biceps EMG electrodes were connected to the analogue inputs of a Lab Rat LR-10 acquisition system (Tucker Davis Technologies, Gainesville, FL). The EMG signals were sampled at approximately 1.5 kHz and high-pass filtered at 300 Hz.

Before insertion, we coated a 16-channel silicon depth electrode (A1x16-3mm-100-177-A16) with fluorescent DiI (Vybrant DiI Cell-Labeling Solution; Life Technologies, Grand Island, NY). Electrodes were inserted using a multiprobe manipulator (New Scale Technologies; Victor, NY) controlled by an Xbox controller (Microsoft, Redmond, WA). The electrode was inserted into cortex until all electrode sites were beneath the dura (approximately 1500 μm). A chlorinated Ag/Ag-Cl wire (0.25 mm diameter; Medwire, Mt. Vernon, NY) inserted into occipital cortex contralateral to the cortical recording sites served as both reference and ground. Neural signals were sampled at approximately 25 kHz. A high-pass filter (0.1 Hz) and a harmonic notch filter (60, 120, and 180 Hz) were applied.

Electrophysiological data were acquired continuously for 3-6 h using SynapseLite (Tucker Davis Technologies). The Mobile HomeCage enabled stable head-fixation throughout the recording session while rats could freely locomote, groom, and sleep.

Video Collection and Synchronization. As described previously (Dooley et al., 2020), video data were synchronized to electrophysiological recordings so that we could better quantify movements and behavioral state. Rats were surrounded by a clear enclosure within the Mobile HomeCage, enabling unimpeded visual access. The video was recorded using a single Blackfly-S camera (FLIR Integrated Systems; Wilsonville, Oregon) positioned at a 45° angle (relative to the pup's head) and centered on the right forelimb, contralateral to the M1 recordings. This angle provided an unobstructed view of the right whiskers, forelimb, hindlimb, and tail. Video was collected in SpinView (FLIR Integrated Systems) at 100 frames/s, with a 7 ms exposure time and 720- x 540-pixel resolution.

Video frames were synchronized to the electrophysiological record using an external time-locking stimulus. A red LED, controlled by SynapseLite (Tucker Davis Technologies), was in view of the camera and pulsed every 3 s for a duration of 100 ms. Custom MATLAB scripts determined the number of frames between each LED pulse to check for dropped frames. Although infrequent, when the number of frames between pulses was not equal to 300 (3 s inter-pulse interval x 100 frames/s), a "dummy frame" was inserted in that location. This ensured that the video and electrophysiological data were synchronized to within one frame (10 ms) throughout data collection.

Histology. At the end of the recording session, the pup was euthanized with ketamine/xylazine (10:1; >0.08 mg/kg) and perfused with 0.1 M phosphate-buffered saline (PBS) followed by 4% paraformaldehyde (PFA). The brain was extracted and post-fixed in 4% PFA for at least 24 h and was then transferred to a 30% sucrose solution at least 24 h before sectioning.

To confirm the electrode's location in M1, the neocortex was either flattened and sectioned tangentially to the pial surface or sectioned coronally. When sectioned tangentially, the right cortical hemisphere was dissected from the subcortical tissue and flattened between two glass slides (separated using a 1.5 mm spacer) for 5-15 min. Small weights (10 g) applied light pressure to the upper slide. Regardless of the plane of section, the tissue was sectioned at 80 μm. Wet-mounted sections were imaged at 2.5x using a fluorescent microscope and digital camera (Leica Microsystems, Buffalo Grove, IL) to identify the location of the DiI.

Cortical sections were stained for cytochrome oxidase (CO), which reliably delineates both primary sensory areas in cortex at these ages (Seelke et al., 2012). Briefly, cytochrome C (3 mg per 10 mL solution; Sigma-Aldrich), catalase (2 mg per 10 mL solution; Sigma-Aldrich) and 3,3'-diaminobenzidine tetrahydrochloride (DAB; 5 mg per 10 mL solution; Spectrum, Henderson, NV) were dissolved in a 1:1 dilution of PB-H2O and distilled water. Sections were developed in well plates on a shaker at 35–40°C at approximately 100 rotations per min for 3–6 h, after which they were washed in PBS, mounted onto glass slides, and allowed at least 48 h to dry. Once dry, sections were placed in citrus clearing solvent (Richard-Allan Scientific) and cover slipped.

RN sections were stained using cresyl violet, which reliably delineates the large cell bodies in RN from the surrounding tissue (Rio-Bermudez et al., 2015). On mounted gelatin-coated slides, sections were dehydrated via submersion in increasing concentrations of ethanol in distilled water for 5-min each. Sections were then defatted using two 5-min washes of citrus clearing solution (Richard-Allan Scientific), followed by a rinse in 100% ethanol. Sections were then stained in a 0.1% cresyl violet solution for 5-10 min, rinsed in distilled water, and immersed in a differentiation solution (70% ethanol with 0.1-0.5% acetic acid) until cell nuclei were maximally differentiated. Finally, sections were fully dehydrated in 100% ethanol for 5-min, followed by 5-min in 2 subsequent rinses of citrus clearing solvent, and cover slipped.

Stained sections were photographed at 2.5x or 5x magnification. Multiple photographs were combined into a single composite image (Microsoft Image Composite Editor; Microsoft, Redmond, WA) and the electrode location were visualized in relation to areal, nuclear, and laminar boundaries of the stained tissue.

Classification of Behavioral State. As described previously, behavior, nuchal EMG signals, and cortical LFP were used to identify periods of wake, active sleep, and quiet sleep (Dooley et al., 2021). Wake was characterized by periods of high nuchal muscle tone and wake-related behaviors (e.g., locomotion, grooming). Active sleep was characterized by the occurrence of myoclonic twitches against a background of muscle atonia. At P16 and later, active sleep was also accompanied by the presence of continuous theta oscillations in thalamic and RN recordings. During quiet sleep, we observed high cortical delta power, behavioral quiescence, and moderate nuchal muscle tone, although periods of high delta power were sometime accompanied by nuchal muscle atonia. Periods not assigned as active or quiet sleep were designated as wake. Active wake was defined as that part of the wake period that was within 3 s of a wake movement.

Classification of Movement. As described previously (Dooley et al., 2021), to quantify periods of movement, we used custom MATLAB scripts to detect frame-by-frame changes in pixel intensity within regions-of-interest (ROIs). The number of pixels within the ROI that exhibited an intensity change >5% were summed. This calculation was performed for each frame, resulting in a 100 Hz time series of changes in pixel intensity which was used to identify periods of movement.

For twitches, the movement timeseries for a ROI containing the body part of interest (e.g., forelimb) was visualized alongside the video using Spike2 (Version 8; Cambridge Electronic Design, Cambridge, UK). Peaks in the time series were confirmed to be

twitches of the appropriate body part. Twitch onset was defined as the first frame in which movement occurred (using the ROI timeseries data described above). For the forelimb, hindlimb, and tail, this method effectively counted every visible twitch, since even twitches in rapid succession have distinct onset and offset times. However, for whisker twitches, alternating protractions and retractions did not always have clear temporal boundaries, thus making it difficult to determine when one whisker twitch ended, and another began. In these instances, only the first whisker twitch in a series of twitches was counted.

For wake movements, an ROI of the entire animal was used. Multiple wake movements typically occur in quick succession; however, we wanted to be sure that every labeled wake movement identified a transition from no movement to movement. Thus, we often marked the first wake movement in a bout of wake movements.

Local Field Potential. For all local field potential analyses, the raw neural signal was down sampled to ~1000 Hz and smoothed using a moving Gaussian kernel with a half-width of 0.5 ms.

Quantification and statistical Analysis

Spike Sorting. SynapseLite files were converted to binary files using custom MATLAB scripts and sorted with Kilosort2.0 (Pachitariu et al., 2016). Briefly, data were whitened (covariance-standardized) and band-pass filtered (300-5000 Hz) before spike detection. Template-matching was implemented to sort the event waveforms into clusters. The first-pass spike detection threshold was set to six standard deviations below the mean and the second-pass threshold was set to five standard deviations below the mean. The minimum allowable firing rate was set to 0.01 spikes/s and the bin size for template detection was set to 262,400 sample points, or approximately 11 s. All other Kilosort parameters were left at their default values.

Clusters were visualized and sorted in Phy2 (Rossant and Harris, 2013). Putative single units had spike waveforms that reliably fit within a well-isolated waveform template, appeared in a principal component analysis as a distinct cluster, and had an auto-correlogram with a decreased firing rate at a time lag of 0 (indicative of a unit's refractory period).

Clusters meeting the first two criteria but not the third were considered multi-units and were discarded from analysis. Any putative unit with a waveform template indicative of electrical noise, a firing rate < 0.01 spikes/s, or amplitude drift across the recording period was discarded. Cross-correlograms of all single- and multi-units on nearby channels were compared. If cross-correlograms and auto-correlograms were similar, clusters were merged and (if appropriate) reclassified as multi-units.

Determination of Twitch-Responsiveness. All analyses of neural data were performed in MATLAB using custom-written scripts. The relation between neural activity and twitches was assessed as follows. First, all twitches of each body part (forelimb, hindlimb, whiskers, tail) were behaviorally scored. For each body part that had more than 20 twitches, perievent histograms of neural activity were constructed (window size: -3 to 3 s; bin size: 10 ms). Next, we determined the mean baseline firing rate from -3 to -0.5 s. Finally, we z-scored the perievent histograms by subtracting the baseline from the raw

perievent histograms and dividing this value by the standard deviation of the baseline. A neuron was considered “responsive” to twitches if it showed a clear peak with a z-score of at least 3.5 for at least one body part.

To accurately determine a neuron’s preferred somatotopic response, we only analyzed twitches for a given body part that were separated by at least 100 ms from twitches of other body parts. The preferred body part for each neuron was the body part with the largest peak in the z-scored perievent histogram. At all ages, neurons in the forelimb region of M1 responded to RFL twitches, not RHL, tail, or whisker twitches.

Movement Analysis. For each movement type (twitches of different body parts and wake movements), we calculated the average displacement produced by that movement for each pup. To ensure subsequent twitches (of the same or different body parts) did not influence the average displacement of a twitch, for this analysis, we used the same subset of twitch triggers used in the somatotopy analysis above (i.e., twitches with inter-twitch-intervals of at least 100 ms). Median average displacement was calculated over all triggered twitches (or wake movements) at each timepoint. Because the size of the ROI used to assess movements varied across age and body part, median values for each animal were always normalized.

Width at Half-Height. To measure width at half-height, the neural data were first smoothed using a 5-bin kernel and then upscaled from 10 ms bins to 1 ms bins using the interp1() function in MATLAB. The data were then normalized so that the baseline was equal to 0 and the peak was set to 1. The width at half-height (in ms) was calculated as the number of continuous bins greater than 0.5 around the peak of the normalized data.

Proportion of spikes before twitch onset. The proportion of spikes before movement onset was calculated by approximating the integral of z-scored perievent histograms triggered on twitch onset using the trapz() function in MATLAB. First, a window was selected that was inclusive of period of elevated activity for the neurons being analyzed (-0.2 to 0.75 s for the M1 development analysis, and -0.2 to 0.2 s for the M1-RN analysis). The proportion of activity before twitch onset was calculated by dividing the integral from -0.2 to 0 s by integral of the entire window. For three neurons, a negative value in the numerator produced a nonsensical negative proportion of spikes. Thus, for these neurons the proportion was set to 0.

Statistical Analyses. All statistical tests were performed using MATLAB. Alpha was set at 0.05 for all analyses; when appropriate, the Bonferroni procedure was used to correct for multiple comparisons. Unless otherwise stated, mean data are always reported with their standard error (SE). Data were tested for significance using a one-way ANOVA, two-way ANOVA, or t test. Categorical data were tested for significance using a Chi-squared test.

Violin plots were constructed absent outliers, which were determined using the isoutlier() function in MATLAB. This function excludes datapoints that are more than three scaled median-absolute-deviations from the median.

Results

Features of REM and NREM sleep in M1 activity through P24

To establish whether REM-sleep twitches continue to drive activity in M1 beyond P12, we recorded single-unit activity in head-fixed, unanesthetized rats at P12, P16, P20, and P24. Several experimental details encouraged REM sleep on the day of testing. First, rats were tested in the Mobile HomeCage, allowing rats to freely locomote (**Figure 1A**). Second, we increased the temperature of the recording environment to about 29 degrees Celcius (Szymusiak and Satinoff, 1981). This allowed us to capture significant periods of REM and NREM sleep at all ages (**Figure 1B**). Extracellular activity was recorded in the forelimb region of M1 (P12: N = 9 pups, 121 neurons; P16: N = 12 pups, 177 neurons; P20: N = 12 pups, 172 neurons; P24: N = 8 pups, 87 neurons). Neural activity, electromyographic activity of the nuchal and biceps muscles, and high-speed video (100 frames/s) were recorded continuously for 3-6 h, and representative data from each behavioral state and each age can be seen in **Figure 2**. Recordings were performed entirely during the lights-on period (1000 to 1700 hours).

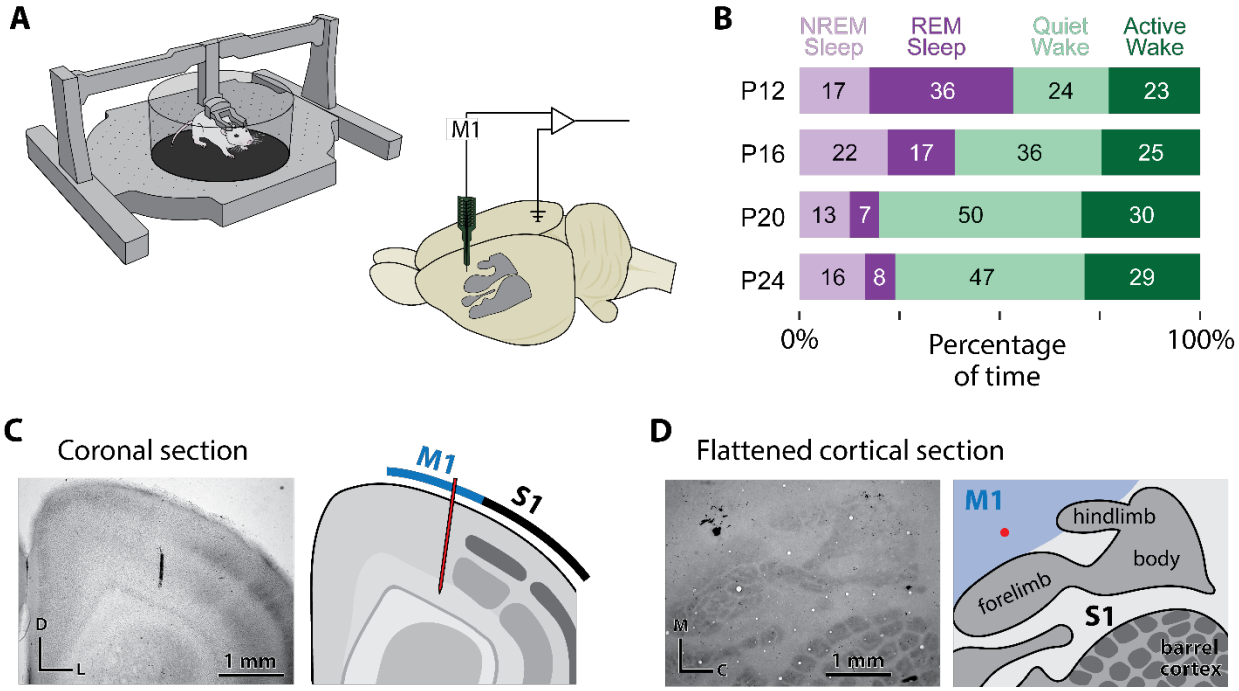

Figure 1. Recording environment, sleep staging, and histological verification of M1 recordings
(A) Left: An illustration of the Mobile HomeCage used to record behavioral and electrophysiological data from head-fixed rat pups across sleep and wake. Right: A schematic of the rat brain with the primary somatosensory cortex (S1) shaded in gray, highlighting the approximate recording location in M1 (circle) and the reference/ground in the contralateral occipital cortex.
(B) Mean percentage of time spent in REM sleep (dark purple), NREM sleep (light purple), quiet wake (light green), and active wake (dark green) at each age. Numbers in each bar indicate the percentage of total recording time for that state.
(C) Representative coronal section stained for cytochrome oxidase showing the DiI-labeled electrode track in M1.
(D) Representative flattened cortical section stained for cytochrome oxidase showing the DiI-labeled electrode track in M1. Borders of primary somatosensory cortex are shown; the DiI-labeled track is visible in the forelimb region of M1.

All rats cycled between NREM sleep, REM sleep, and wake throughout the recording sessions, and as expected, the percentage of time spent in REM sleep decreased across age, whereas the percentage of time spent in quiet wake increased (see **Figure 1B**). Consistent with prior work, NREM sleep was associated with increased delta power (1-4 Hz) relative to quiet wake at all ages tested (**Figure 3 left**; Seelke and Blumberg, 2008). At P16, P20, and P24, NREM sleep in M1 also showed an increase in alpha (8-15 Hz) power, likely reflecting the developmental emergence of sleep spindles, which in humans first appear postnatally (Robert, 1982 p.198; Sokoloff et al., 2021). REM sleep showed a markedly different oscillatory profile. Relative to periods of quiet wake, REM sleep in P12 pups was associated with a general increase in power across all frequencies. In P16, P20, and P24 pups, periods of REM sleep showed an increase in theta (4-8 Hz) power, and a decrease in Delta and Alpha bands, as well as an increase in slow gamma (**Figure 3 right**). The developmental emergence of theta power in M1 between P12 and P16 was also evident in the raw power spectrum; increased power in the theta band was not present at P12, but was present at P16, P20, and P24 (**Figure S1**).

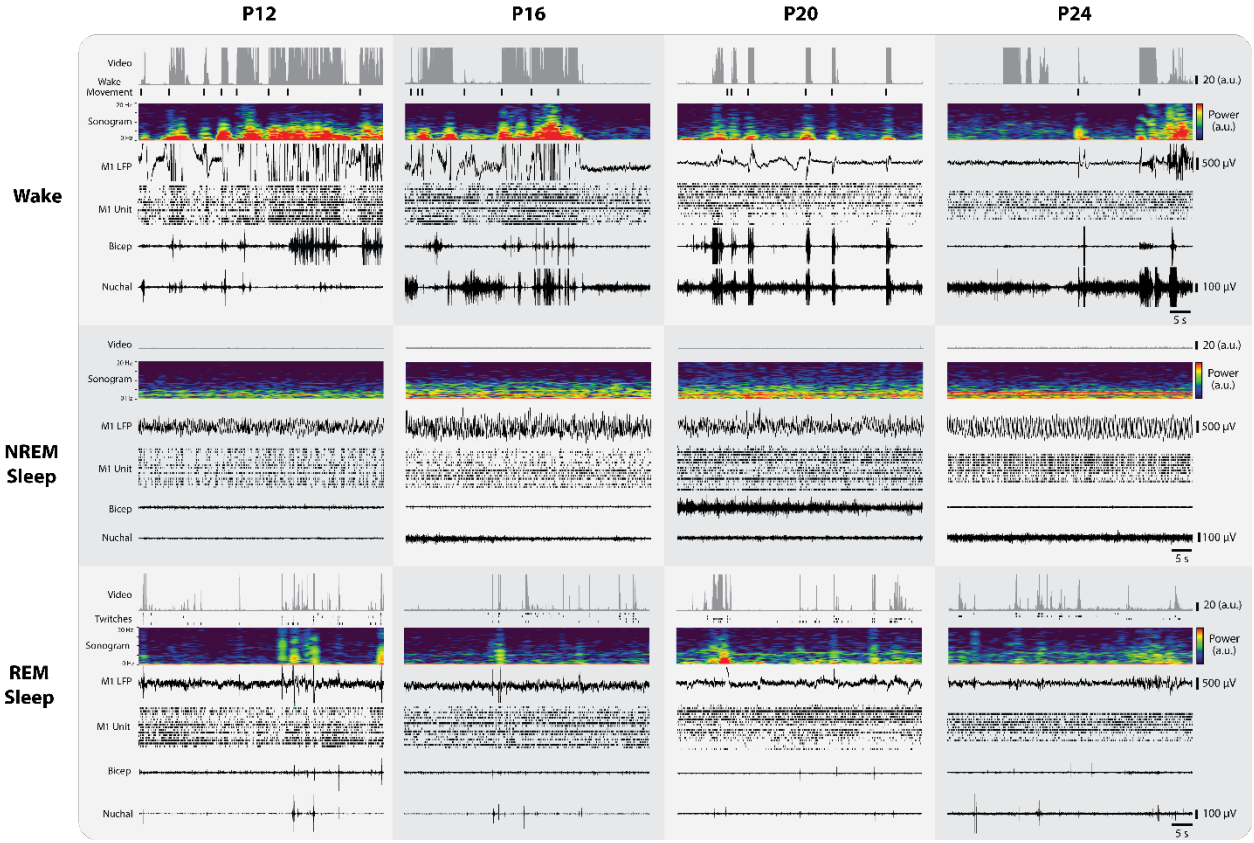

Figure 2. Representative behavioral and electrophysiological data across wake, NREM sleep, and REM sleep

For each age (P12, P16, P20, P24), a 50-s segment of continuous data is shown for (top to bottom) wake, NREM sleep, and REM sleep. The following data **(top to bottom)** is shown in each 50-s segment: Video-based movement analysis (as detected by pixel-based motion detection), scored twitches and wake movements, M1 LFP, single-unit activity in M1 (each row corresponds to a separate unit), and biceps and nuchal EMG signals. These representative examples demonstrate distinct patterns of behavioral, neural, and muscular activity at each developmental age.

We observed a change in the rate of M1 activity by age during wake ($F_{(3,553)} = 6.51$; $p < 0.0005$), NREM sleep ($F_{(3,433)} = 8.2$; $p < 0.0001$), and REM sleep ($F_{(3,553)} = 3.56$; $p < 0.05$; **Figure S2A**). Directly comparing neural activity during wake and REM sleep, we observed more activity during REM sleep than wake at P12 ($t_{120} = 9.278$, $p < 0.0001$), P16 ($t_{176} = 6.55$, $p < 0.0001$), and P20 ($t_{171} = 8.23$, $p < 0.0001$), but not P24 ($t_{86} = 1.20$, $p = 0.23$; **Figure S2B**). The disappearance of this state-dependent difference in activity at P24 may be why previous studies in adult rodents have not reported more activity during REM sleep compared to wake, as it suggests that the increase in cortical activity during REM sleep is developmentally transient.

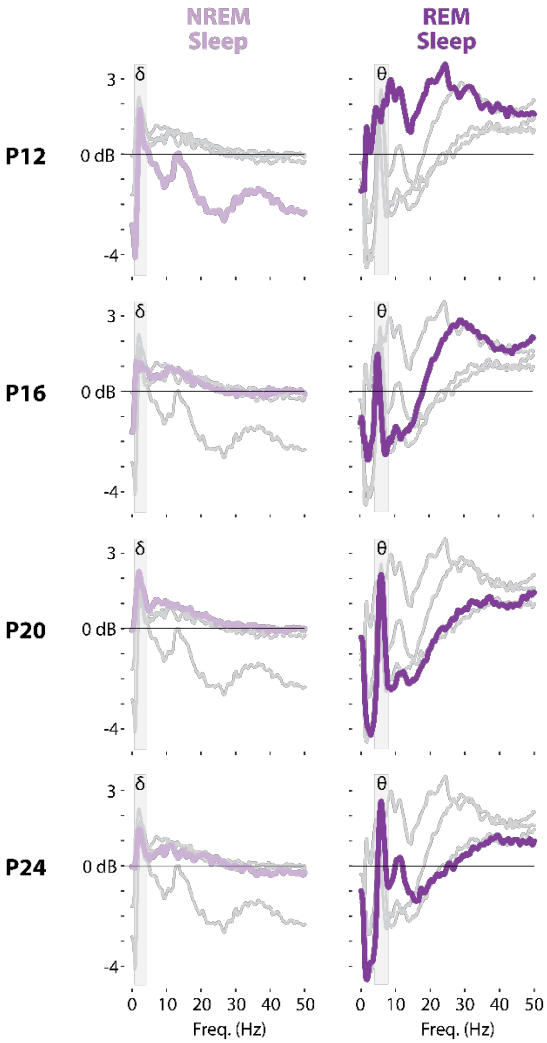

Figure 3. Developmental changes in oscillatory power during NREM and REM sleep
Normalized power spectra (1–50 Hz) at each age (P12, P16, P20, P24) are plotted relative to quiet wake. **(Left)** NREM sleep (light purple) exhibits a pronounced delta peak at all ages. **(Right)** REM sleep (dark purple) demonstrates an emerging theta peak from P16 onward. For each panel, data for the focal age are highlighted in color, whereas spectra for the other three ages are shown in gray for comparison. These findings illustrate the marked developmental changes in low-frequency (delta) and mid-frequency (theta) oscillations across sleep states.

Temporal refinement of twitch-related activity from P12 to P24

Over half of M1 neurons responded to forelimb movements during wake and/or forelimb twitches during REM sleep (P12: 77%; P16: 74%; P20: 55%, P24: 65%; **Figure 4A**). At P12, a greater proportion of M1 neurons responded to twitches than wake movements, but at P16 and beyond, more M1 neurons responded to wake movements than twitches, and only a small minority of neurons that were twitch responsive were not wake responsive (**Figure 4B**). This is not surprising, as wake movements are much longer in duration than twitches, and unlike twitches, involve the simultaneous activation of

numerous muscles. Still, at all ages examined, over a quarter of movement-responsive neurons in M1 responded to twitches. Representative twitch responsive neurons at each age can be seen in **Figure 4C**.

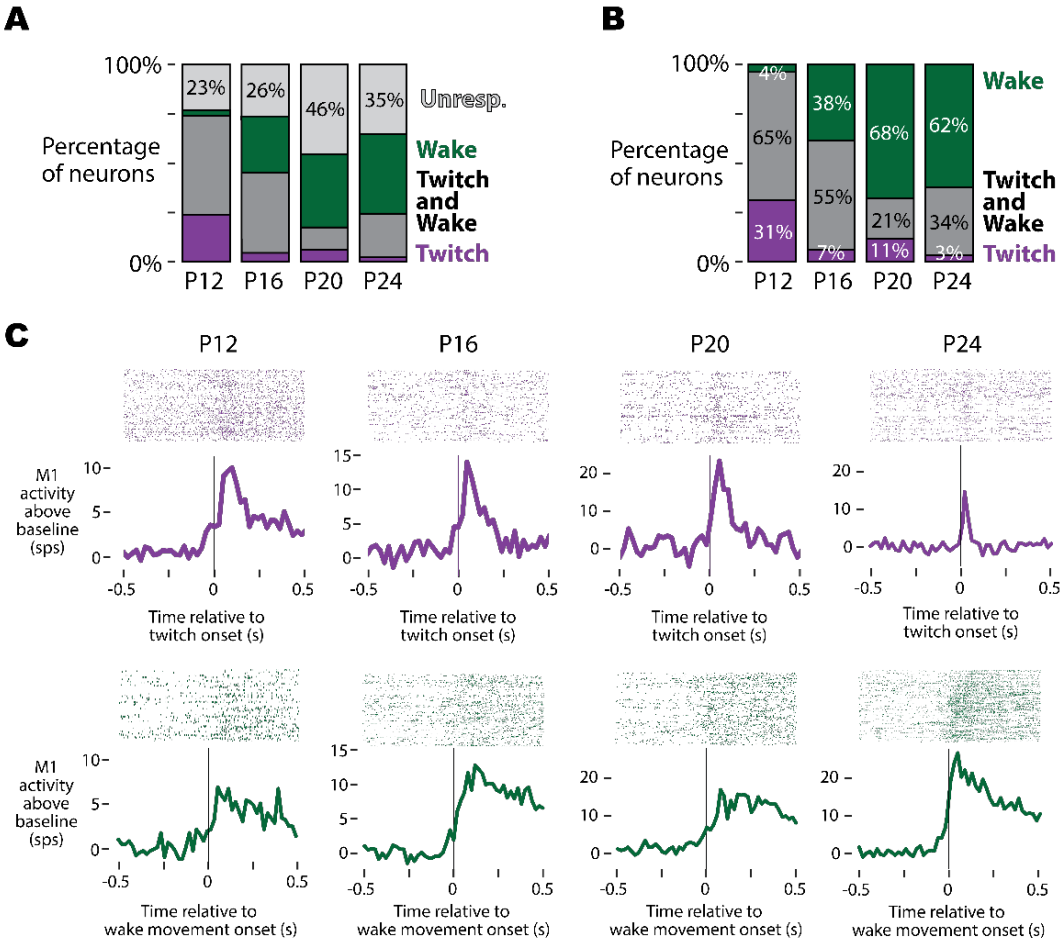

Figure 4. Movement responsiveness in M1 neurons across development
(A) Stacked bar plots showing the percentage of M1 neurons at each age (P12, P16, P20, P24) that respond to self-generated movements (i.e., twitches during REM sleep or wake movements).
(B) Of the movement-responsive neurons identified in (A), the percentage that respond to twitches (purple), wake movements (green), or both (gray) are shown in stacked bars for each age.
(C) Representative M1 neurons from each age (P12, P16, P20, P24), illustrating raster plots (top) and perievent histograms (bottom) triggered on twitch onset (purple) or wake movement onset (green). Each histogram depicts firing rate changes relative to baseline, demonstrating robust but developmentally evolving movement-related activity in M1.

At a population level, although movement-responsive neurons did show some variability, twitch- and wake-movement-related activity was quite similar within an age (**Figure 5A, B**). However, twitch-responsive neurons in M1 showed temporal refinement across age, mirroring a similar finding in sensory and motor thalamus at these ages (Dooley et al., 2021). As evidence of this refinement, the width at half-height of twitch-responsive neurons varied significantly with age ($F_{(3,209)} = 60.4$; $p < 0.0001$), with older ages generally showing briefer responses to twitches compared to younger ages (**Figure 5C**). In addition, the time of the peak response also varied significantly with age ($F_{(3,305)} = 7.28$;

p < 0.0001); again older animals showed earlier peak activity than younger animals (**Figure 5D**), such that at P20 and P24, the timing of peak M1 responses more closely resembled the timing observed in the ventral lateral nucleus ("motor" thalamus) than the ventral posterior nucleus of thalamus (see Dooley et al., 2021). We next calculated the proportion of twitch-related activity that occurred before twitch onset across ages (**Figure 5E**). This proportion increased significantly with age ($F_{(3,216)} = 30.5$; $p < 0.0001$), from a mean proportion of 0.10 at P12 to a mean proportion of 0.22 and 0.20 at P20 and P24, respectively. Thus, by P20, about 20% of activity in M1 precedes movement onset.

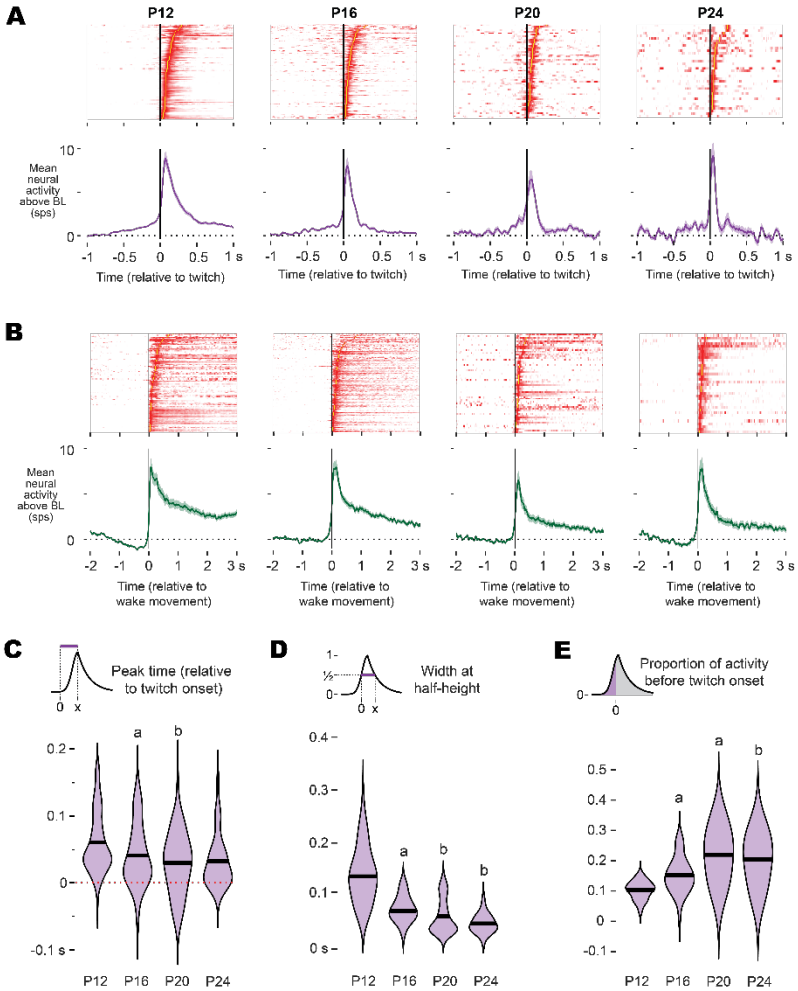

Figure 5. Temporal refinement of twitch- and wake-related M1 activity with age
(A) Top: Heatmaps showing twitch-triggered responses of all twitch-responsive M1 neurons across P12, P16, P20, and P24. Each row corresponds to a single neuron, and color intensity indicates firing rate. Bottom: Mean (±SEM) perievent histograms of these neurons for each age.
(B) Same as (A), but for wake-triggered responses of M1 neurons.
(C) Violin plots of the peak response time (relative to twitch onset) for twitch-responsive M1 neurons by age. The black line represents the mean of the distribution. 'a' indicates a significant difference from the preceding age, whereas 'b' indicates a significant difference from two ages prior.
(D) Same as (C), but for the width at half-height of twitch-triggered responses.
(E) Same as (C), but for the proportion of twitch-related activity that precedes movement. Collectively C-E reveals progressive temporal sharpening of M1 responses to twitches over the course of development.

Twitches are discrete movements, often involving only a single muscle at a time. Because of this, we were able to use these movements to examine whether M1 shows somatotopic precision at these ages. We scored twitches of the right forelimb, right hindlimb, whiskers, and tail. This enabled us to trigger M1 neural activity on temporally-isolated twitches of all 4 of these body parts (i.e. forelimb twitches that do not occur alongside twitches of the hindlimb, whiskers, or tail). All of our M1 recordings were the region of M1 that shows forelimb movement-related activity in adults (the caudal forelimb area). Our data show that, at all ages examined (P12 to P24), twitch-responsive neurons in the forelimb region of M1 only respond to forelimb twitches (**Figure S3**). This suggests that at least course somatotopy is present in M1 by P12.

By focusing on the population of twitch-responsive neurons in M1, we observed that only a small proportion of neurons in M1 showed activity that categorically preceded movement onset (see **Figure 5A**). This suggests that, through P24, M1's role in motor production remains limited. This finding is consistent with previous reports that have used ICMS to assess M1 motor output (Young et al., 2012; Singleton et al., 2021). However, across these ages, we did observe an increase in the proportion of twitch-related activity that precedes movement onset (see **Figure 5E**), suggesting that by P24, movement-related activity in M1 may be beginning to resemble activity seen in a traditional motor structure. To better contextualize this transition, we next compared activity in M1 of P24 rats with activity in RN, the midbrain motor nucleus believed to be responsible for movements, including twitches, throughout infancy (Williams et al., 2014; Rio-Bermudez et al., 2015).

RN activity precedes twitches and wake movements at P24

Prior work demonstrates that RN generates forelimb twitches through at least P12 (Rio-Bermudez et al., 2015), and work on M1 and RN interactions suggests that RN's role in motor control persists through the developmental emergence of M1 motor control (Williams and Martin, 2015). Thus, RN is presumed to be responsible for forelimb twitches through P24, although this has yet to be confirmed experimentally. To confirm RN's role in movement production, and to compare the activity of M1 to a motor structure, we performed dual recordings in M1 and RN of P24 rats (**Figure 6A, B**; N = 7 animals; 112 Neurons in M1; 111 Neurons in RN). In RN, baseline firing rates significantly differed across REM sleep and wake ($t_{110} = 8.86$, $p < 0.0001$) with RN firing nearly twice as much during REM sleep ($\bar{x} = 13.1$ spikes/s) than during wake ($\bar{x} = 7.2$ spikes/s; **Figure 6C**).

A majority of RN neurons from P24 rats showed an increase in activity during forelimb movements (RN: 60%; **Figure 6D**). 61% of the forelimb-responsive neurons showed twitch related activity, whereas 85% showed wake-movement related activity (**Figure 6D**). A representative RN neuron showing twitch and wake-movement related activity is shown in **Figure 6E**. Movement-related activity in RN was much more heterogeneous than was seen previously in M1, particularly with respect to wake movements. For example, whereas some twitch-responsive RN neurons showed movement-related activity for nearly every wake movement (see **Figure 6E**), other twitch-responsive RN neurons showed no activity—or even inhibition—during wake movements.

Upon closer examination, some of the RN neurons that appeared to show no wake-movement-related activity had a bifurcated response (**Figure S4, A, D**), such that a subset of wake movements were accompanied by a burst of activity, while others were accompanied by inhibition (**Figure S4, B, E**). This is not too surprising, as wake movements encompass an incredibly heterogenous mixture of behaviors. If an RN neuron is involved in wake movement production, it is likely for specific movements, similar to the results produced by stimulating neurons in M1 (Peters et al., 2017). For two such neurons, we examined which parts of the body moved for both the responsive and non-responsive

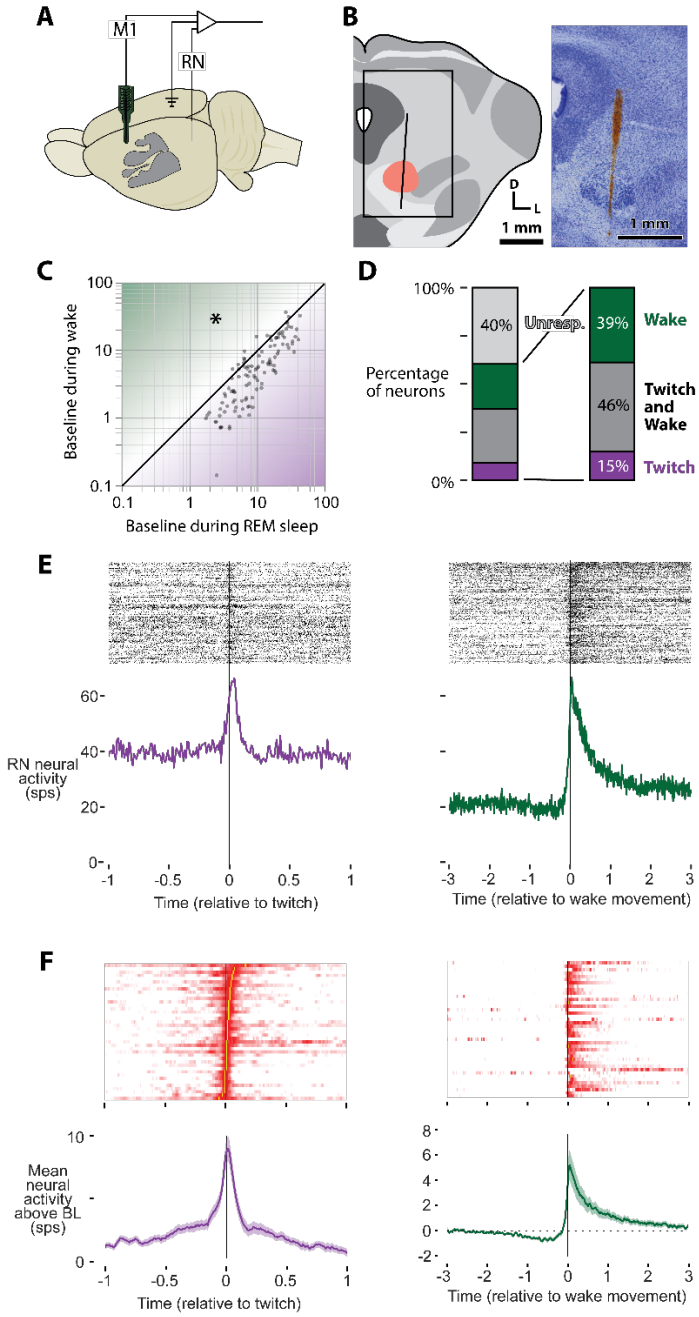

Figure 6. RN recordings and responsiveness to movement at P24
(A) Schematic of the rat brain illustrating the dual recording sites in M1 and RN in P24 rats.
(B) Cartoon representation of a coronal section through the midbrain, showing the RN (red oval) and a representative electrode track for RN recordings. The rectangle on the left indicates the region enlarged on the right, which depicts the Nissl-stained section with the electrode track (red) passing through RN.
(C) Scatter plot of baseline RN neuronal activity during REM sleep (x-axis) versus wake (y-axis). Most RN units exhibit higher firing rates in REM sleep than in wake, and this difference is significant (asterisk).
(D) Stacked bar plots showing the proportion of RN neurons responsive to forelimb movements. The subplots on the right illustrate the fraction of those responsive neurons that react to twitches (purple), wake movements (green), or both (gray). This parallels the format of Figures 4A and 4B for M1.
(E) Representative RN neuron displaying raster plots and averaged perievent histograms for twitch- (top, purple) and wake-movement-triggered (bottom, green) responses.
(F) Heatmaps of all twitch-responsive RN neurons triggered on twitch onset (left) and wake movement onset (right), akin to Figures 5A and 5B for M1.

wake movements. We found that in both cases, the responsive wake movements were more likely to involve the left and right forelimbs ($\chi^2 = 37.9$, N = 454, $p < 0.001$; $\chi^2 = 55.2$, N = 354, $p < 0.001$), and a video-based analysis showed that the responsive wake movements generally involved moving both forelimbs to the face, while the unresponsive wake movements showed no overall pattern (**Figure S4 C, F**). These neurons underscore the heterogeneous nature of RN responses during wake: even within a single RN neuron, some wake movements elicit excitation, whereas others produce inhibition. This variability suggests that a more detailed behavioral categorization of wake movements is necessary to fully capture RN's movement-related activity. At the ages of this investigation, no such diversity of responses was seen in M1.

Movement-related activity in M1 lags RN at P24

The population-level activity seen in this second group of M1 neurons from P24 rats (**Figure 7A**) closely resembles those seen previously (see **Figures 4, 5**). In aggregate, movement-related activity in M1 and RN is similar, with both structures showing brief increases in neural activity surrounding twitches and/or wake movements (**Figure 7B, C top**). However, in RN, twitch-related activity increases earlier than in M1, a difference that is particularly apparent when subtracting normalized twitch-related activity of responsive RN neurons from equivalent M1 neurons (**Figure 7B bottom**). This difference between twitch-related activity in M1 and RN can be exhibited quantitively: In RN, twitch-related activity peaks nearly 20 ms earlier than M1 (t_{98} = -5.18, $p < 0.0001$; **Figure 7D**). Because of this increase in preceding activity, twitch-related activity in RN is broader than in M1

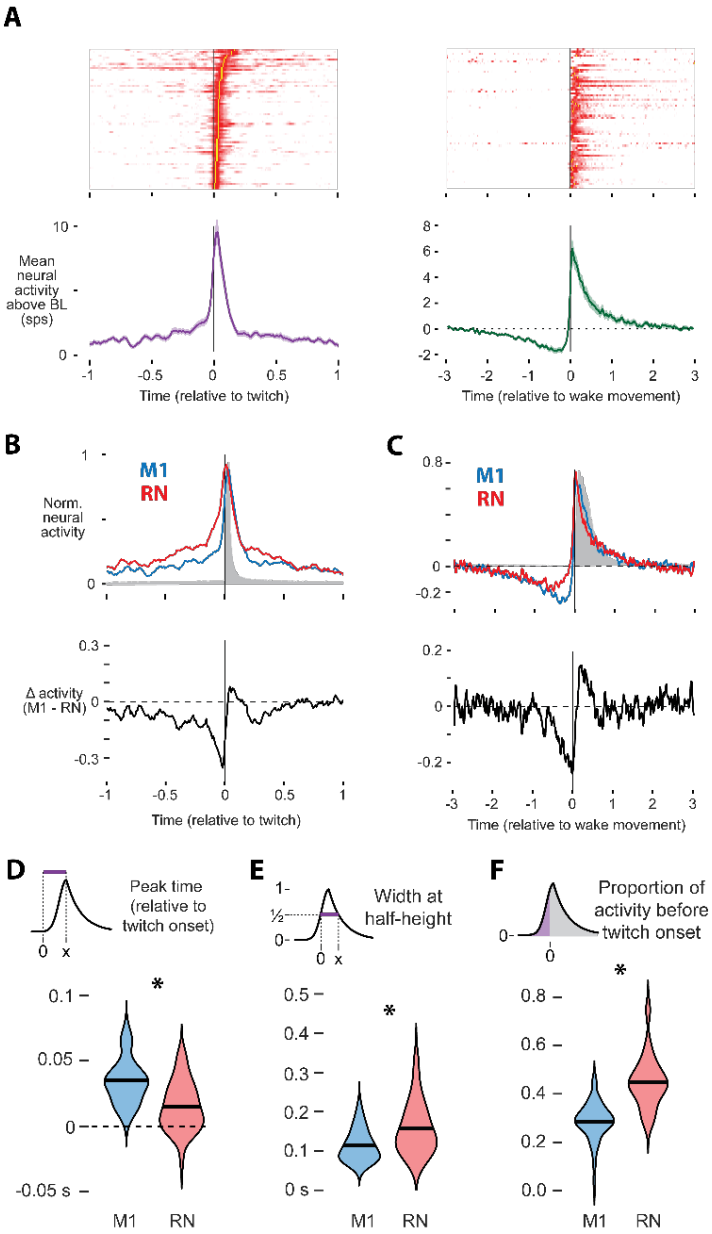

Figure 7. Comparison of twitch- and wake-related activity between M1 and RN at P24

(A) Heatmaps of twitch- (left) and wake-movement-related (right) responses in all twitch-responsive M1 neurons recorded during dual M1–RN recordings (compare to Figure 6F for RN).

(B) Top: Averaged, normalized twitch-triggered firing rates of M1 (blue) and RN (red) neurons. The gray shaded region indicates the period of observed forelimb movement. Bottom: The difference in normalized firing rates (M1 minus RN) shows RN activity precedes M1 activity.

(C) Same as (B), but for wake-triggered movements. Again, RN activity tends to precede or co-occur earlier than M1 activity.

(D) Violin plots of peak twitch-related activity for twitch-responsive M1 (blue) and RN (red) neurons, showing that RN responses peak significantly earlier than those in M1. Asterisk signifies a significant difference between groups.

(E) Violin plots of the width at half-height for neurons that show twitch-related activity, comparing M1 and RN neurons as in (D).

(F) Violin plots of the proportion of activity that precedes twitch onset for neurons that show twitch-related activity, again comparing M1 and RN neurons.

(t_{102} = -4.18, $p < 0.0001$; **Figure 7E**), and a greater proportion of activity in RN preceded twitch onset compared to M1 (0.45 and 0.29, respectively; **Figure 7F**; t_{109} = -8.35, $p < 0.0001$). Thus, as late as P24, RN shows much more preceding activity than M1 and thus is still largely responsible for the production of twitches. Notably, a similar pattern, albeit with less temporal precision, is also observed when comparing aggregate wake-movement-related activity in M1 and RN (**Figure 7C, bottom**), suggesting that RN is also responsible for wake movement production at this age.

Discussion

We have shown here that in P12 to P24 rat pups, neural activity in M1 reliably reflects self-generated movements, including REM-sleep twitches and wake movements. By leveraging the spontaneity and discreteness of twitches, we revealed that M1 is somatotopically refined as early as P12 and maintains robust movement-related activity throughout this developmental period. Further, across these ages, M1's twitch-related responses become increasingly temporally precise. Nevertheless, our simultaneous recordings of neurons in M1 and RN—the subcortical motor nuclei responsible for limb movements in infancy—reveal that in P24 rats, activity in RN precedes both twitches and wake movements to a greater extent than M1. Altogether, our findings fill a critical gap in our understanding of the neural activity that drives M1 through this developmental window. Because this activity largely follows the initiation of subcortically initiated behaviors, our results underscoring the continued reliance of M1 on reafferent signals rather than direct motor control.

The same movements drive different patterns of M1 activity across development

Although infant M1 is not yet producing movement, it is not silent. M1 undergoes several functional transformations prior to assuming its adult role in behavioral production. From near birth through P10, activity in M1 is heavily patterned by twitches, whereas wake-movement-related activity is inhibited, mirroring the broader sensorimotor system's early reliance on reafferent signals from twitches (Khazipov et al., 2004; Tiriac et al., 2014; Tiriac and Blumberg, 2016; Dooley and Blumberg, 2018). From P10 to P12, functional activity in M1 undergoes several changes. The first change is the elimination of the inhibition of wake-movement-related activity; this transition also occurs in the developing somatosensory and visual cortices (Dooley and Blumberg, 2018; Murata and Colonnese, 2018). The second change is in the types of somatosensory inputs that M1 receives. Prior to P12, M1 receives both tactile and proprioceptive inputs from thalamus, in parallel with somatosensory cortex. From P12 onward, M1 only receives proprioceptive inputs from thalamus, becoming reliant on somatosensory cortex for tactile information (Gómez et al., 2021). Finally, population-level activity in M1 goes from bursty to continuous while neurons rapidly decorrelate their sensory responses (Glanz et al., 2021). From the present investigation, we also now know that by P12, M1 shows somatotopic refinement, with the forelimb region of M1 only responding to forelimb twitches (see **Figure S3**).

The present investigation focused on movement-related activity in M1 following the P12 transformation. Prior work on somatosensory and motor thalamus (the ventral posterior and ventral lateral nuclei, respectively) identified P12 to P20 as a period of temporal refinement of movement-related activity (Dooley et al., 2021). Because motor thalamus is the primary thalamic input to M1, it is not surprising that we observed similar temporal refinement in M1 across this developmental window. In addition, by P20, activity in motor thalamus no longer reflects sensory inputs, but instead reflects a cerebellar-dependent internal model of movement. In the present investigation, the mean latency to peak twitch-related activity in M1 of P20 and P24 rats is about 30 ms (see **Figure 5C**)—the same as previously reported in motor thalamus. Thus, by P20, movement-related activity in M1 has likely undergone another transformation: It no longer represents sensory feedback and instead represents a cerebellar-dependent internal model of movement.

Twitches continue to drive activity in M1 through P24

Prior work at earlier ages demonstrated that twitch-related activity in sensorimotor cortex is quite dynamic across early development (Dooley and Blumberg, 2018; Dooley et al., 2021). Whereas limited evidence in adult rodents suggests that REM sleep twitches may drive activity in thalamus (Boscher et al., 2024) and M1 (Eckert et al., 2020), the apparent reduction in the proportion of twitch-responsive neurons in infant sensorimotor cortex (Dooley and Blumberg, 2018; Domínguez et al., 2021; Glanz et al., 2021) has led to the suggestion that the twitch-responsiveness seen in early infancy may be developmentally transient. In line with this notion, our findings reveal that the proportion of twitch-responsive neurons in M1 does decrease from 74% of neurons at P12 to 24% of neurons at P24. This transition, in which M1 neurons shift from responding to twitches to predominantly responding to wake movements, may reflect an expanding range of preferred stimuli as the cortex matures. Indeed, a similar progression—from simple to more complex motor maps—has been documented previously, albeit in rats older than the present investigation (Singleton et al., 2021). Nonetheless, a meaningful portion of M1 neurons retained twitch-related activity through P24.

Critically, this persistence of twitch-related activity in M1 through P24 suggests that twitches continue to play an important role in refining cortical circuits. At this age, activity in M1 is critical to the development of its motor functions (Chakrabarty and Martin, 2005; Williams and Martin, 2015). Thus, this twitch-related reafference likely continues to shape M1's circuitry in preparation for its motor functions. Further, by demonstrating that twitch responsiveness persists, our results leave open the possibility that twitches continue to promote ongoing plasticity through adulthood. Altogether, these results underscore the potential significance of sleep and twitches in facilitating the final stages of M1's developmental transition toward adult-like motor control.

Sensorimotor integration in developing M1

Our data reveals that twitch-related activity in M1 shows increasing temporal precision between P12 and P24, a result made possible because of the discrete and isolated nature of twitches. As wake movements are not as discrete and isolated as twitches, it was not practical for us to measure similar temporal refinement. However, we presume that wake-movement-related neural activity also becomes more precise across this developmental window. Consequently, the varied and coordinated movements of wake likely serve as an effective 'training ground,' pushing M1 to integrate the types of sophisticated movement-related inputs that will characterize its adult functionality.

These results also align with broader principles of experience-dependent plasticity in immature neural circuits. The relatively late developmental onset of M1 motor control is thought to allow experience to play a larger role in its formation, as both sensory feedback and movement-related activity exert a powerful influence on M1's organization and plasticity (Chakrabarty and Martin, 2005; Martin, 2005). Much like activity in somatosensory cortex or other early cortical regions (Martini et al., 2021), M1's reliance on reafferent signals ensures that self-generated behaviors—twitches and wake movements alike—drive the activity that refines its circuitry. By integrating and incorporating more and more complex motor behaviors, M1 is laying the groundwork for future motor control and learning. And the continued role of both wake movements and twitches to this process highlights that M1's developmental trajectory depends on a continuum of sensorimotor experiences across sleep and wake to shape the eventual development of its adult-like motor functions. Whether wake movements and twitches provide different functions to this developmental process remains to be determined.

Developmental transition towards motor control

Our comparison of M1 with the RN underscores a critical distinction between emerging and established motor control structures. For both twitches and wake movements, activity in RN reliably preceded both activity in M1 and the movements themselves. At P24, RN showed significantly more activity preceding movement than M1 (see **Figure 7**). This is consistent with RN's role in generating forelimb behaviors during early development (Williams et al., 2014; Rio-Bermudez et al., 2015; Williams and Martin, 2015). Whereas neural activity in M1 did not consistently lead forelimb movements, we did observe individual neurons—particularly at P20 and P24—whose twitch-related activity markedly preceded movement onset, suggesting that at these ages, some M1 neurons may be on the verge of driving behavior. This shift aligns with previous electrophysiological and ICMS studies showing that M1's capacity to produce discernible motor outputs begins around P25, at which point cortical stimulation of small—but expanding—region of M1 produces forelimb movements (Young et al., 2012; Singleton et al., 2021).

This gradual emergence of M1-driven behaviors highlights that "motor control" at these ages relies on a delicate interplay between early descending corticospinal projections and

the still-dominant subcortical output systems, represented in this study by RN. Whereas ICMS studies suggest that onset of M1 motor control is P25, it takes until around P60 before M1's forelimb motor map appears "adult-like" (Young et al., 2012; Singleton et al., 2021). However, even these motor map milestones are subject to debate regarding what exactly they represent functionally, as some evidence suggests that the formation and reorganization of motor maps lags behind changes of the underlying circuitry (Kleim et al., 2004; Peters et al., 2017). Accordingly, it is plausible that discrete, behaviorally meaningful motor outputs from M1 begin earlier than can be detected via ICMS, and that the progressive refinement we observe in twitch-related M1 activity serves as a key developmental step leading to more robust cortical control.

Taken together, our findings support a dynamic model in which M1's influence on motor output begins to emerge in parallel with continued subcortical support from RN. This interplay between M1 and RN likely reflects both the gradual maturation of corticospinal projections and the essential role of early reafferent signals in sculpting motor circuitry (Martin, 2005). Indeed, the incremental "pre-movement" activity we observe at P20 and P24 may be the first glimpse of M1's ability to shape behavior. As M1's descending pathways strengthen, wake movements, together with twitches, contribute to the final transition wherein cortical control increases—and eventually—becomes dominant.

References

Boscher F, Jumel K, Dvořáková T, Gentet LJ, Urbain N (2024) Thalamocortical Dynamics during Rapid Eye Movement Sleep in the Mouse Somatosensory Pathway. J Neurosci 44 Available at: https://www.jneurosci.org/content/44/25/e0158242024 [Accessed January 3, 2025].

Chakrabarty S, Martin JH (2005) Motor but not sensory representation in motor cortex depends on postsynaptic activity during development and in maturity. J Neurophysiol 94:3192–3198.

Domínguez S, Ma L, Yu H, Pouchelon G, Mayer C, Spyropoulos GD, Cea C, Buzsáki G, Fishell G, Khodagholy D, Gelinas JN (2021) A transient postnatal quiescent period precedes emergence of mature cortical dynamics Nelson SB, Moore T, Nelson SB, Colonnese MT, eds. eLife 10:e69011.

Dooley JC, Blumberg MS (2018) Developmental “awakening” of primary motor cortex to the sensory consequences of movement. Elife 7.

Dooley JC, Glanz RM, Sokoloff G, Blumberg MS (2020) Self-Generated Whisker Movements Drive State-Dependent Sensory Input to Developing Barrel Cortex. Curr Biol 30:2404-2410.e4.

Dooley JC, Sokoloff G, Blumberg MS (2021) Movements during sleep reveal the developmental emergence of a cerebellar-dependent internal model in motor thalamus. Curr Biol.

Eckert MJ, McNaughton BL, Tatsuno M (2020) Neural ensemble reactivation in rapid eye movement and slow-wave sleep coordinate with muscle activity to promote rapid motor skill learning. Philos Trans R Soc B Biol Sci 375:20190655.

Glanz RM, Dooley JC, Sokoloff G, Blumberg MS (2021) Sensory Coding of Limb Kinematics in Motor Cortex across a Key Developmental Transition. J Neurosci 41:6905–6918.

Gómez LJ, Dooley JC, Sokoloff G, Blumberg MS (2021) Parallel and Serial Sensory Processing in Developing Primary Somatosensory and Motor Cortex. J Neurosci 41:3418–3431.

Inagaki HK, Chen S, Ridder MC, Sah P, Li N, Yang Z, Hasanbegovic H, Gao Z, Gerfen CR, Svoboda K (2022) A midbrain-thalamus-cortex circuit reorganizes cortical dynamics to initiate movement. Cell 185:1065-1081.e23.

Kawai R, Markman T, Poddar R, Ko R, Fantana AL, Dhawale AK, Kampff AR, Olveczky BP (2015) Motor cortex is required for learning but not for executing a motor skill. Neuron 86:800–812.

Khazipov R, Sirota A, Leinekugel X, Holmes GL, Ben-Ari Y, Buzsáki G (2004) Early motor activity drives spindle bursts in the developing somatosensory cortex. Nature 432:758–761.

Kleim JA, Hogg TM, VandenBerg PM, Cooper NR, Bruneau R, Remple M (2004) Cortical synaptogenesis and motor map reorganization occur during late, but not early, phase of motor skill learning. J Neurosci Off J Soc Neurosci 24:628–633.

Lopez-Virgen V, Macías M, Rodriguez-Moreno P, Olivares-Moreno R, de Lafuente V, Rojas-Piloni G (2023) Motor cortex projections to red and pontine nuclei have distinct roles during movement in the mouse. Neurosci Lett 807:137280.

Martin JH (2005) The corticospinal system: From development to motor control. The Neuroscientist 11:161–173.

Martini FJ, Guillamón-Vivancos T, Moreno-Juan V, Valdeolmillos M, López-Bendito G (2021) Spontaneous activity in developing thalamic and cortical sensory networks. Neuron 109:2519–2534.

Mukherjee D, Yonk AJ, Sokoloff G, Blumberg MS (2017) Wakefulness suppresses retinal wave-related neural activity in visual cortex. J Neurophysiol 118:1190–1197.

Murata Y, Colonnese MT (2018) Thalamus Controls Development and Expression of Arousal States in Visual Cortex. J Neurosci 38:8772–8786.

Pachitariu M, Steinmetz N, Kadir S, Carandini M, Kenneth D. H (2016) Kilosort: realtime spike-sorting for extracellular electrophysiology with hundreds of channels. bioRxiv:061481.

Peters AJ, Liu H, Komiyama T (2017) Learning in the rodent motor cortex. Annu Rev Neurosci 40:77–97.

Rio-Bermudez CD, Sokoloff G, Blumberg MS (2015) Sensorimotor Processing in the Newborn Rat Red Nucleus during Active Sleep. J Neurosci 35:8322–8332.

Robert JE (1982) Development of Sleep Spindle Bursts During the First Year of Life. Sleep 5:39–46.

Rossant C, Harris KD (2013) Hardware-accelerated interactive data visualization for neuroscience in Python. Front Neuroinform 7:36.

Ruder L, Schina R, Kanodia H, Valencia-Garcia S, Pivetta C, Arber S (2021) A functional map for diverse forelimb actions within brainstem circuitry. Nature 590:445–450.

Sauerbrei BA, Guo JZ, Cohen JD, Mischiati M, Guo W, Kabra M, Verma N, Mensh B, Branson K, Hantman AW (2020) Cortical pattern generation during dexterous movement is input-driven. Nature 577:386–391.

Seelke AM, Blumberg MS (2008) The microstructure of active and quiet sleep as cortical delta activity emerges in infant rats. Sleep 31:691–699.

Seelke AM, Dooley JC, Krubitzer LA (2012) The emergence of somatotopic maps of the body in S1 in rats: the correspondence between functional and anatomical organization. PLoS One 7.

Singleton AC, Brown AR, Teskey GC (2021) Development and plasticity of complex movement representations. J Neurophysiol 125:628–637.

Sokoloff G, Dooley JC, Glanz RM, Wen RY, Hickerson MM, Evans LG, Laughlin HM, Apfelbaum KS, Blumberg MS (2021) Twitches emerge postnatally during quiet sleep in human infants and are synchronized with sleep spindles. Curr Biol 31:3426–3432.

Szymusiak R, Satinoff E (1981) Maximal REM sleep time defines a narrower thermoneutral zone than does minimal metabolic rate. Physiol Behav 26:687–690.

Tiriac A, Blumberg MS (2016) Gating of reafference in the external cuneate nucleus during self-generated movements in wake but not sleep. Elife 5.

Tiriac A, Del Rio-Bermudez C, Blumberg MS (2014) Self-generated movements with “unexpected” sensory consequences. Curr Biol 24:2136–2141.

Williams PT, Martin JH (2015) Motor Cortex Activity Organizes the Developing Rubrospinal System. J Neurosci 35:13363–13374.

Williams PTJA, Kim S, Martin JH (2014) Postnatal maturation of the red nucleus motor map depends on rubrospinal connections with forelimb motor pools. J Neurosci Off J Soc Neurosci 34:4432–4441.

Yang L, Martin JH (2023) Effects of motor cortex neuromodulation on the specificity of corticospinal tract spinal axon outgrowth and targeting in rats. Brain Stimulat Available at: https://www.sciencedirect.com/science/article/pii/S1935861X23017540 [Accessed April 26, 2023].

Yang W, Kanodia H, Arber S (2023) Structural and functional map for forelimb movement phases between cortex and medulla. Cell 186:162-177. e18.

Young NA, Vuong J, Teskey GC (2012) Development of motor maps in rats and their modulation by experience. J Neurophysiol 108:1309–1317.